J Mater Sci: Mater Med (2010) 21:2213–2226
DOI 10.1007/s10856-010-4081-x

Friction transfer of polytetrafluoroethylene (PTFE) to produce nanoscale features and influence cellular response in vitro

V. R. Kearns · P. J. Doherty · G. Beamson · N. Martin · R. L. Williams

Received: 4 November 2009 / Accepted: 6 April 2010 / Published online: 24 April 2010

Abstract A large number of cell types are known to respond to chemical and topographical patterning of substrates. Friction transfer of polytetrafluoroethylene (PTFE) onto substrates has been shown to produce continuous, straight, parallel nanofibres. Ammonia plasma treatment can be used to defluorinate the PTFE, decreasing the dynamic contact angle. Fibroblast and epithelial cells were elongated and oriented with their long axis parallel to the fibres, both individually and in clusters. The fibres restricted cell migration. Cell alignment was slightly reduced on the plasma-treated fibres. These results indicated that although surface topography can affect cellular response, surface chemistry also mediates the extent of this response.

1 Introduction

The response of eukaryotic cells to the chemical and topographical features of substrates has been well-studied. Many cell types exhibit contact guidance, both to culture substrates in vitro and biological structures in vivo. Much of the early research on contact guidance focussed on the production of micron-scale grooves on substrates and the subsequent response of a variety of cell types to these topographies (reviewed [1–3]). More recently, features in the nanometre range, both chemical and topographical, have been found to induce orientation of a variety of cell types [4–6]. Recent work has reported that features on the nanoscale can reduce the spreading and proliferation of mammalian cells [7] and affect differentiation [8]. Several reviews on nanopatterning of biomaterial substrates and its effect on cellular response are available [9] and the potential applications to medical devices have been discussed by Curtis et al. [10].

A variety of techniques can be used to produce nanoscale features on biomaterial substrates (reviewed [11]). Friction transfer is one such technique reported to produce features in the nanoscale. This process involves the transfer of a material, usually a polymer, to a smooth, flat surface when the two materials are rubbed together. Polytetrafluoroethylene, PTFE, is the most commonly studied polymer for friction transfer. Under a variety of conditions, a thin film or series of fibres are deposited onto a substrate. Friction transfer of PTFE has been successfully performed onto a variety of substrate types including silicon wafers [12, 13] and glass [14]. Three parameters that affect the nature of the PTFE transferred to the substrate are the temperature of the substrate and the PTFE [12, 15], the pressure exerted on the substrate by the PTFE [12–14] and the speed at which the PTFE is traversed across the substrate [16]. These three parameters interact to cause localised melting of the PTFE at the polymer-substrate interface, which allows transfer of the molten polymer to the substrate. In low friction regimes such as those used in this study, sliding speed is reported to have no significant effect on the transfer film [14].

V. R. Kearns (✉) · P. J. Doherty · R. L. Williams
Clinical Sciences, University of Liverpool,
Liverpool L69 3GA, UK
e-mail: vkearns@liverpool.ac.uk

G. Beamson
STFC Daresbury Laboratory, Daresbury,
Cheshire WA4 4AD, UK

N. Martin
School of Clinical Dentistry, University of Sheffield,
Sheffield S10 2TA, UK

PTFE has high thermal stability, low surface energy and is chemically inert. This makes it ideal for many industrial applications but means that it is very difficult to alter its surface chemistry or add functional groups without altering the bulk properties of the polymer. One of the few ways in which this can be done is by gas plasma treatment. Ammonia plasma treatment defluorinates the surface of the PTFE [17] and often leads to the incorporation of oxygen- and nitrogen-containing groups, which can be stabilised by post-treatment in an aqueous solution [18]. The helical resonator plasma (HRP) system used in these studies has been comprehensively investigated in terms of its use for ammonia plasma treatment of PTFE and other polymers [17, 19]. These studies have resulted in the development of a protocol for plasma-treatment and post-treatment of PTFE which was used in this study.

A few studies have examined protein adsorption onto PTFE films including sub-fragments of myosin molecules [20] and fibrinogen [21]. On 30 nm wide PTFE fibres, fibrinogen molecules were oriented in a perpendicular manner to the long axis of the fibres, whereas on 600 nm wide fibres, a fibrinogen network was formed. To date, no literature is available on the cellular response to friction-transferred PTFE films. The aim of this study was to firstly investigate the conditions required to produce friction transferred PTFE nanofibres on glass substrates and the effect of ammonia plasma treatment on fibre chemistry and topography and secondly to study the effect of nanoscale surface variations in chemistry and topography, and their combination, on in vitro cellular response.

2 Methods

2.1 Manufacture of substrates

The substrates were glass microscope slides (VWR International Ltd., UK) (for characterisation studies), glass coverslips (VWR) (for cell studies) or silicon wafers [for X-ray photoelectron spectroscopy (XPS)]. Prior to friction transfer, substrates were rinsed with isopropanol and allowed to air dry. An apparatus that allowed the variation of substrate temperature, PTFE temperature and applied pressure was used to perform friction transfer. This apparatus and its operation have been described previously [13]. In brief, substrates were placed on the heating block (pre-heated to the desired temperature) and left for at least 5 min to reach thermal equilibrium. A PTFE (Goodfellow, UK) blade was traversed across the substrate via the motorised stage under the required load at a constant speed of 0.6 mm s^{-1}. A summary of manufacturing conditions can be found in Table 1.

Table 1 Summary of manufacturing conditions

Manufacturing condition	Substrate temperature (°C)	Pressure (kPa)
1	200	0.5
2	200	1.2
3	200	1.9
4	200	2.5
5	225	1.2
6	225	1.9
7	225	2.5
8	250	1.2
9	250	1.9
10	250	2.5

2.1.1 Manufacturing conditions

The substrates were subsequently ammonia plasma treated with an in-house built HRP system, with a resonant frequency of 13.56 MHz. This system and its operation have been described previously [19] and the operating conditions have been optimised to defluorinate the surface while causing minimal surface etching [22]. Immediately following plasma treatment, substrates were immersed in de-ionised, UV-sterilised water for at least 12 h. This has been shown to introduce polar groups to the surface [18].

2.2 SEM

Substrates were sputter coated with chromium using an Emitech K575x with a chromium target (125 mA for 4 min). These were then imaged using a LEO 1550 field emission SEM using the secondary electron or in-lens detector, an accelerating voltage of 5 or 10 keV and a working distance of approximately 8–10 mm.

2.3 White light interferometry

Substrates were examined using an NT3300 white light interferometer and associated Vision 32 software (Veeco Instruments, USA). Prior to examination, substrates were sputter coated with chromium (as described above) to ensure high reflectivity and evenness of the reflective index of the substrate surface. Substrates were analysed with the fibre direction running horizontally across the field of view using the 50× objective and the 2× magnifier in vertical scanning interferometry (VSI) mode. The field of view was approximately 60 μm × 45 μm and data were collected over a height range of 10 μm (this height range comfortably exceeded the height range of the surface features). Data from 27 fields of view were captured from each substrate: 24 from the fibre-coated areas and 3 from the

uncoated glass at the edges of the substrate. The height profile in the direction perpendicular to the fibre direction was captured. Five height profiles were obtained from each field of view and from these, surface profile parameters were calculated. These were the roughness average (R_a), root mean square roughness (R_q), skewness (R_{sk}) and kurtosis (R_{ku}).

2.4 Dynamic contact angle measurement

Pairs of substrates were glued together to give double-thickness substrates. The outside surface of these substrates was the test surface, with fibre-coated substrates being oriented such that the fibres were running the same direction on both sides. The water dynamic contact angles (DCA) of the substrates were measured using a Dynamic Contact Angle Analyzer DCA-322 and software (Cahn). All substrates were dried before analysis. The substrates were immersed into a clean beaker of double-distilled water at a rate of 0.3 mm s^{-1} until 12 mm of the sample was immersed, and then withdrawn at the same rate. The advancing and receding contact angles were determined from the obtained force/immersion curves by the software. For each type of substrate, five replicate samples were tested. The majority of measurements on fibre-coated substrates were undertaken with the substrates oriented such that the fibre direction was vertical. Some measurements were carried out with the fibre direction being horizontal and with uncoated, single-thickness substrates.

2.5 X-ray photoelectron spectroscopy

Untreated and plasma-treated substrates were analysed using a Scienta ESCA300. This employs a high power rotating anode and monochromatised Al Kα X-ray source ($hv = 1{,}486.7$ eV), high transmission electron optics and a multichannel detector [23, 24]. Substrates were examined as described previously [13]. Briefly, the X-ray source was operated at 14 kV, 100 mA (1.4 kW) for survey and region scans. Survey spectra were recorded at 150 eV pass energy and 1.9 mm slitwidth, whereas region spectra were recorded at 150 eV pass energy, 0.8 mm slitwidth. Quantification of the region scans was performed using the ESCA300 data analysis software with straight line backgrounds and elemental sensitivity factors determined from measurements on standard materials of known stoichiometry.

2.6 Cell culture

Fibroblast and epithelial cell lines were maintained under standard conditions. Cells were grown to 80% confluence then detached from the surface using 0.05% trypsin–EDTA. The desired cell number was pipetted onto substrates in a concentrated solution and substrates incubated for 60 min at 37°C. Wells were then flooded with culture medium. Human gingival fibroblasts, HGF-1 (CRL-2014, LGC Promochem, UK), were seeded at 4.5×10^3 cells per substrate and incubated for up to 10 days. Gingival epithelial cells, KB (CCL-17, LGC Promochem, UK), were seeded at 5×10^4 cells/substrate and incubated for 4 days.

For light microscopy and image analysis, substrates were fixed and stained with 0.05% methylene blue. Images were captured on an Axioplan II microscope using an Axiocam colour camera and Axiovision software (Carl Zeiss, Welwyn Garden City, UK). For scanning electron microscopy, substrates were fixed in 2.5% glutaraldehyde for 30 min. Substrates were then dehydrated for 30 min in each of 70, 90 and 100% ethanol. Substrates were placed overnight in a desiccator then sputter coated with chromium (125 mA for 2 min).

2.7 Image analysis

Substrates were seeded with HGF-1 and fixed at 1, 4 and 7 days and substrates seeded with KB and fixed at 4 days were subjected to quantitative image analysis. Live images were captured using a Carl Zeiss Jenaval microscope and transferred to the KS400 (Carl Zeiss, Welwyn Garden City, UK) image analysis software via a JVC 3 chip CCD camera. Colour images were captured and converted to grey scale images and inverted using grey values. Images were segmented to give a binary image and background artefacts (size 10 pixels or less) were eliminated before the data were captured. The data included information on the ratio of width to length of each cell or group of cells (shape ratio) and the angle of the longitudinal axes of cells or groups of cells compared to the horizontal axis of the field of view. For fibre-coated samples, the substrates were placed on the microscope stage and the CCD camera adjusted so that the fibre direction was as close to parallel with the horizontal axis of the field of view as possible. Information for ten fields of view was captured for each substrate. Three replicate substrates were analysed for each condition.

Data were exported to Microsoft Excel® where angles were converted from values in the range 0–180° to a range of 0–90° using the symmetry of the sine function then subsequently analysed in SPSS 14.0 software. The Kolmogorov–Smirnov Z test was used to explore differences in distribution. Skewness and kurtosis were calculated by SPSS® software (v.12 SPSS Inc.). One-way ANOVA and a Games-Howell post-hoc or independent samples t test analyses were used to examine differences between the means of the ratio of cell width to length. The P value considered to represent a significant difference was lowered to $P \leq 0.0025$ for instances where the same data were analysed twice. Correlations between the shape ratio and

angle of cell orientation were calculated using Spearman rank-order correlation.

3 Results

3.1 SEM

Analysis of scanning electron micrographs showed that PTFE was transferred onto the substrates by the friction transfer procedure. When a pressure of 1.2 MPa or higher was applied during manufacture, the deposited PTFE was in the form of continuous, straight, parallel fibres. Fibre widths and spacing were irregular but fibre widths were mostly <200 nm and frequently fibre widths <100 nm were observed. At a substrate temperature of 200 and 225°C, fibres were discrete and the uncoated spaces between fibres were relatively large compared to the fibre widths (Fig. 1a). At the highest substrate temperature, 250°C, these fibres appeared to cover the majority of the surface and were more close-packed (Fig. 1b). There were often groups of close-packed fibres that had little or no space between them. No obvious change in fibre morphology, width or distribution was observed when the pressure was increased from 1.2 to 2.5 MPa. An applied pressure of approximately 0.5 MPa resulted in the deposition of PTFE in streaks and wavy fibres (Fig. 1c). No further investigation of these manufacturing conditions was undertaken. Manufacturing condition 7 (Table 1) was chosen for subsequent cell culture studies as qualitative assessment showed a relatively even distribution of fibres and moderate coverage of the substrates by the coating.

Comparison with untreated, fibre-coated substrates showed that the plasma-treatment did not appear to have altered the fibre coating in terms of topography (Fig. 1d).

3.2 Light interferometry

Comparison of the height profiles obtained using AFM and light interferometry showed that the two techniques generated similar data (data not shown), although the data from light interferometry were noisier. Semi-quantitative assessment of 3-dimensional (3-D) (Fig. 2a) and 2-D (Fig. 2b) height profiles suggests that the majority of fibres were in the 5–25 nm height range; it was not possible to determine absolute values for the height of individual fibres due to the difficulty of ascertaining where the lowest point of the fibre was. Values for surface roughness of the fibre-coated substrates (R_a, R_q and R_{sk}, calculated from height profiles) were low for manufacturing conditions 2–10 (condition 1 was not analysed), being less than 5 nm in the case of R_a and R_q and less than 0.6 for R_{sk}. These values are sufficiently low that the surface could be considered an optical flat, however fibres could be visualised, indicating that surface roughness statistics may be unsuitable for characterising these surfaces.

Fibres could be visualised from light interferometry data from the plasma-treated surfaces. Comparison of plasma-

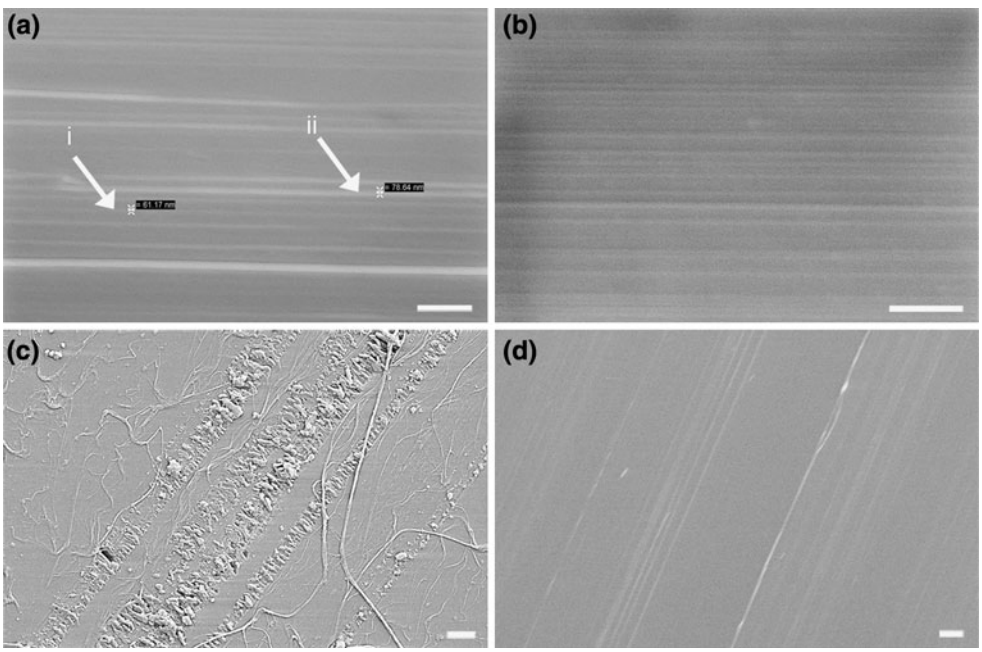

Fig. 1 SEM micrographs of substrates manufactured using different manufacturing conditions (**a**–**c**) and following ammonia plasma treatment (**d**). **a** Condition 2; *scale bar* represents 1 μm; fibre '*i*' 61 nm wide, fibre '*ii*' 79 nm wide. **b** Condition 10; *scale bar* represents 1 μm. **c** Condition 1; *scale bar* represents 2 μm. **d** Condition 7, plasma-treated substrate; *scale bar* represents 10 μm

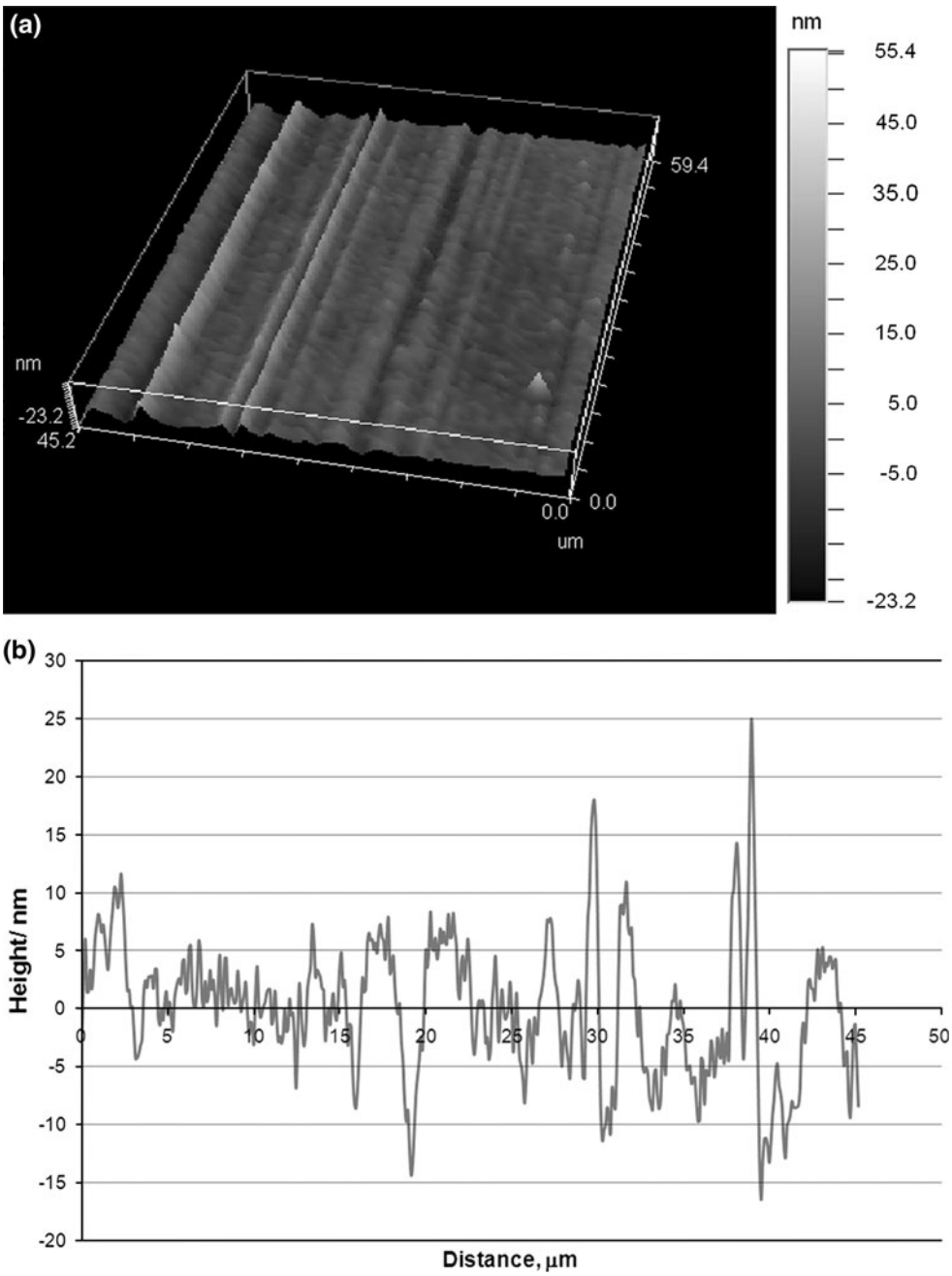

Fig. 2 **a** 3-Dimensional white light interferometry plot of fibre-coated area of substrate and **b** 2-dimensional plot of the substrate shown in **a**

treated substrates and untreated, fibre-coated substrates showed that the plasma-treated substrates had significantly lower values for R_q and R_a (Mann–Whitney U test, $P \leq 0.01$), however the values for both types of surface were very low. There was no difference between the values for R_{sk} ($P = 0.507$).

3.3 DCA

Statistical analysis (one-way ANOVA and R–E–G–W Q post-hoc test, $P \leq 0.05$) showed that single-thickness uncoated substrates appeared to have lower advancing and receding DCA than double-thickness uncoated substrates. It was not possible to calculate advancing or receding contact angles when the substrates were evaluated with the fibres oriented horizontally to the liquid surface as the fibres caused pinning of the contact line resulting in unreliable force measurement (data not shown). When the substrates were oriented so that the fibres were vertical, however, the shape of the force curve allowed a contact angle to be calculated. Mean advancing and receding angles for substrates are shown in Fig. 3. The mean advancing angle on untreated fibre-coated substrates was significantly lower than on untreated uncoated substrates

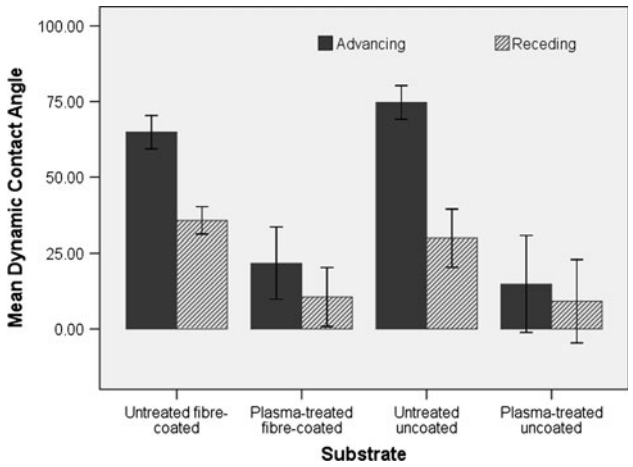

Fig. 3 Dynamic contact angle values for double-thickness, untreated and plasma-treated fibre-coated and uncoated glass control substrates. *Error bars* represent the 95% confidence interval

($P \leq 0.01$), but there was no significant difference in receding angles ($P = 0.17$). This demonstrated that the hydrophobic PTFE fibres have a wicking effect drawing the water up the plate between the fibres by capillary action. The large error bars are likely to be a consequence of the surface roughness. Plasma-treatment reduced the advancing and receding contact angles on fibre-coated and uncoated glass substrates; pairwise comparisons using a Mann–Whitney *U* test confirmed that advancing and receding angles were lower on plasma-treated, fibre-coated substrates than untreated, fibre-coated substrates ($P \leq 0.01$) and that advancing and receding angles were lower on plasma-treated uncoated glass substrates than untreated uncoated glass substrates ($P \leq 0.05$).There was no significant difference in advancing ($P = 0.36$) or receding angles ($P = 0.82$) between uncoated and fibre-coated plasma-treated glass substrates, suggesting that the wicking effect was reduced by the plasma treatment.

3.4 XPS

XPS survey spectra showed fluorine peaks generated from the PTFE, carbon peaks from the PTFE and hydrocarbon contamination and silicone peaks from the Si wafer substrate (Fig. 4a). Oxygen peaks were generated from the Si wafer, or, for plasma-treated substrates, from the plasma

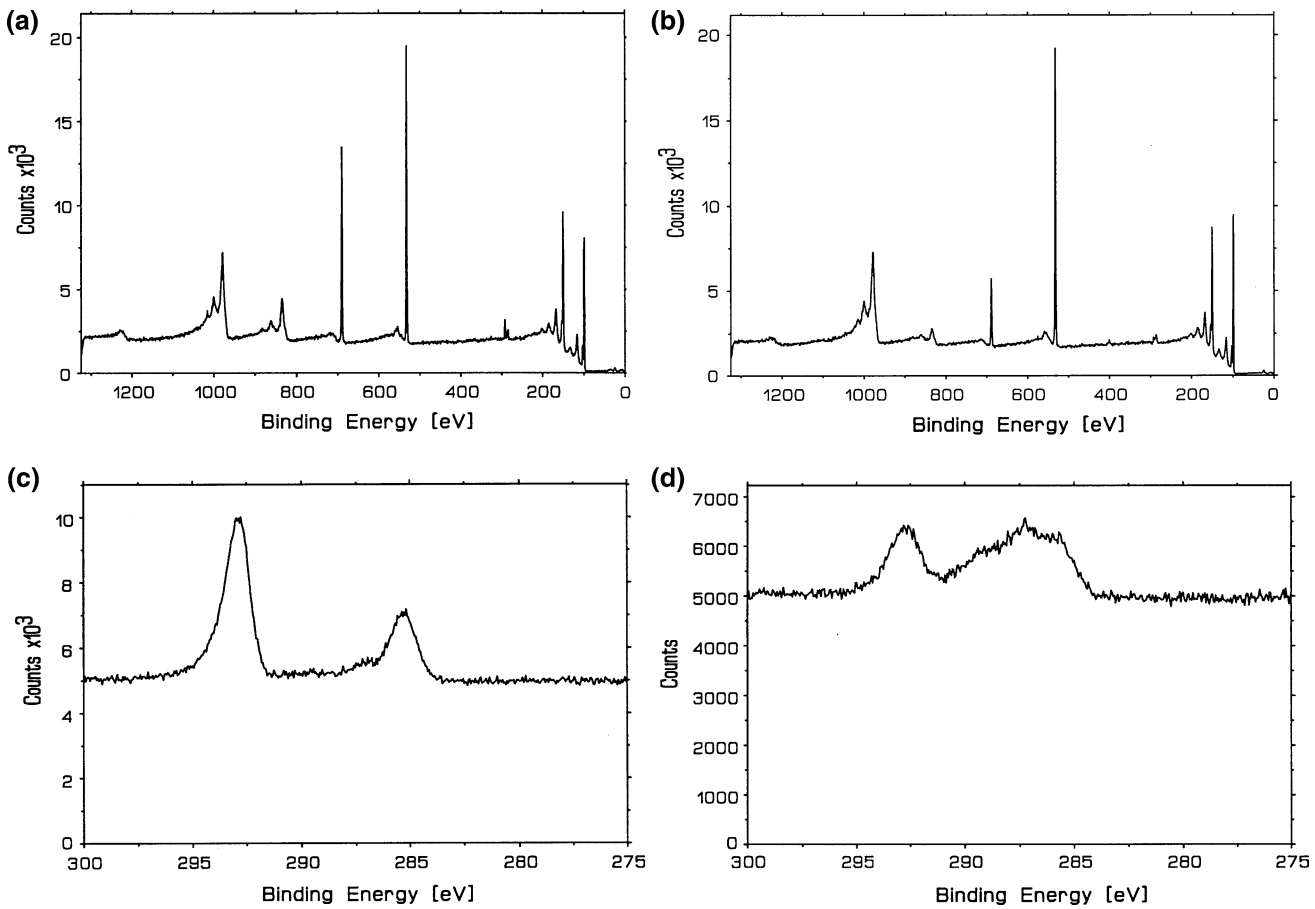

Fig. 4 XPS survey (**a**, **b**) and C1s region (**c**, **d**) spectra for fibre-coated silicon wafer substrates. Untreated (**a**, **c**) substrates show relatively high fluorine and C–F peaks compared to ammonia plasma-treated substrates (**b**, **d**)

treatment. There was an additional small nitrogen peak observed on the survey spectra for plasma-treated substrates (Fig. 4b), again from the ammonia plasma treatment. It was inferred from quantification of F1s that the amount of fluorine was lower following ammonia plasma treatment. A similar trend was found with C–F quantification. C1s region spectra allowed comparison of C–H and C–F peaks. On untreated substrates (Fig. 4c), the C–F peak (approx 292 eV) was higher than the C–H peak (at 285 eV) and both peaks were sharp. On plasma-treated substrates (Fig. 4d), the shape of the carbon envelope changed significantly. The intensity of the component assigned to C–F was reduced in comparison with the intensity of the component at 285 eV. Furthermore the component at 285 eV was significantly broader after plasma treatment than before suggesting the incorporation of other carbon species as a result of the plasma and post treatment in water. These data correlate well with previous data on the plasma treatment of PTFE [22] and would suggest the presence of oxygen containing carbon species.

3.5 Cellular response

On untreated fibre-coated substrates, some individual HGF-1 cells appeared to be oriented such that their long axis was parallel with the fibre direction after 1 day of growth and continued to be so oriented at all subsequent time points (e.g. Fig. 5a). The proportion of oriented cells appeared to increase with time. Many of the cells had a bi-polar morphology. On plasma-treated, fibre-coated substrates, some cells were observed to be oriented to the fibres but others were not and had stellate morphology. This mixture of oriented and non-oriented cells was repeated at later time points, although the majority of cells appeared to be oriented at 7 days (Fig. 5b). Examination of oriented cells on both types of fibre-coated substrates showed that the cells were well-spread. On uncoated glass substrates, cells were randomly oriented, with a mixture of bi-polar and stellate morphologies (e.g. Fig. 5c). SEM analysis indicated that some cells spread laterally across several fibres, whereas others had straight edges, seemingly abutting a fibre edge. Cell processes appeared to contact the substrate between the fibres.

KB cells grew in clusters on fibre-coated substrates. Cells growing within the cluster exhibited typical cobblestone epithelial morphology (Fig. 6a). Clusters were elongated in the fibre direction after 1 day of growth and at all subsequent time points, indicating that the cells were proliferating and migrating preferentially in the fibre direction. Cells growing individually (i.e. not within clusters) were bipolar, with their long axes running in the fibre direction. When examined at higher magnification (Fig. 6b), cells on the edge of clusters were seen to have straight edges

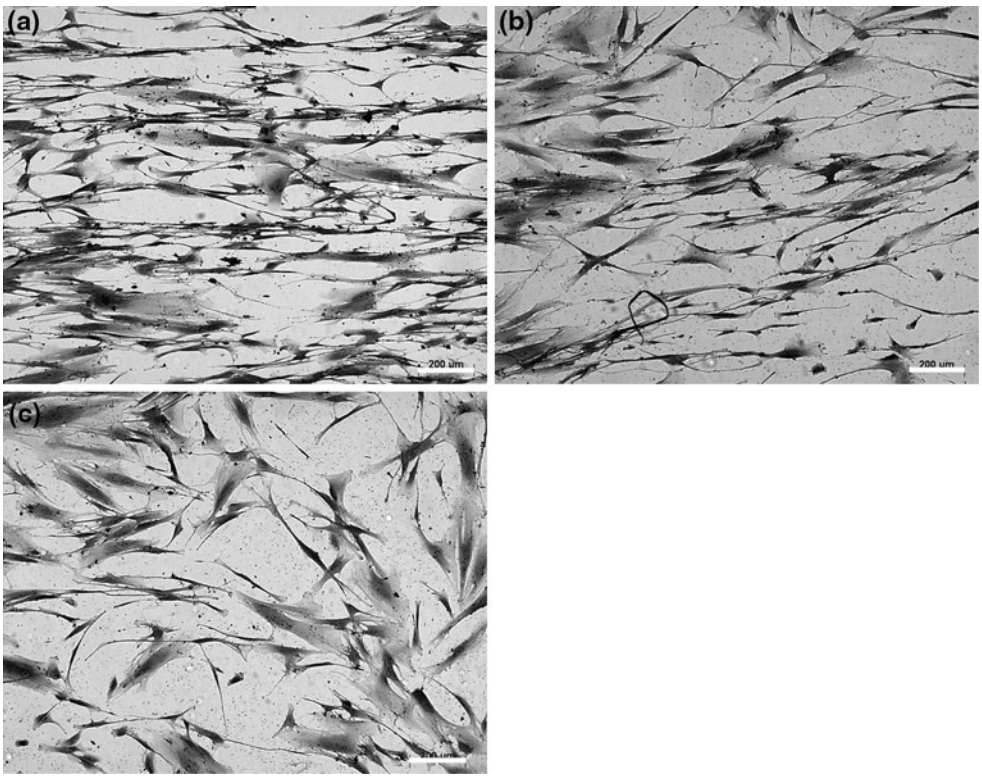

Fig. 5 HGF-1 on (**a**) untreated fibre-coated, (**b**) plasma-treated fibre-coated and (**c**) uncoated substrate stained after 7 days. Fibre direction for fibre-coated substrates approximately horizontal. *Scale bar* represents 200 μm

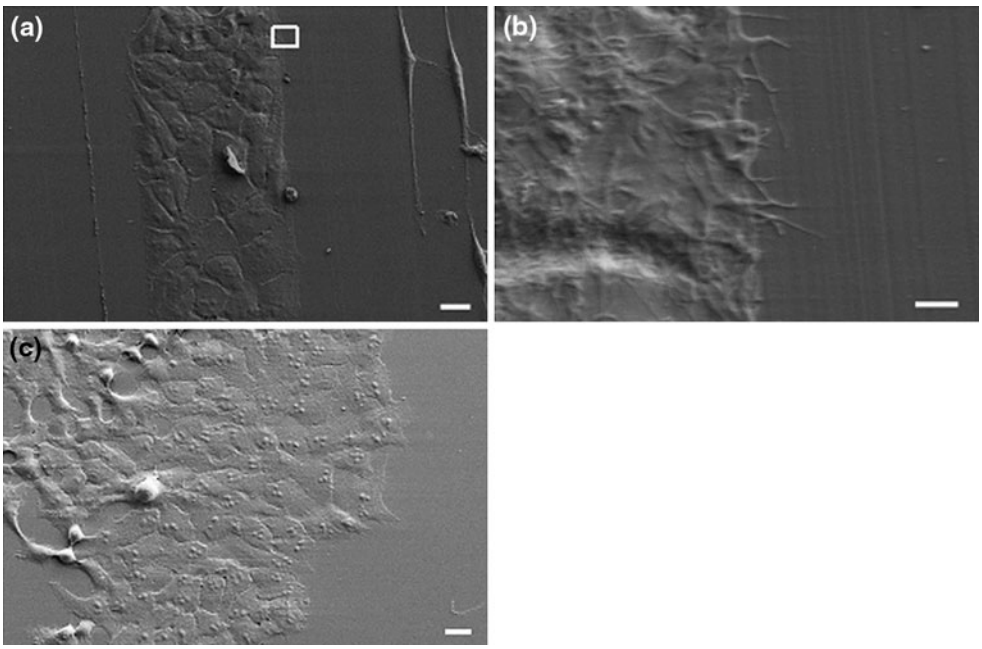

Fig. 6 SEM micrograph of KB cells grown on (**a**, **b**) fibre-coated and (**c**) uncoated substrate for 4d. Fibre direction approximately vertical. (**b**) Represents a higher magnification image of the area indicated in (**a**). *Scale bar* represents 20 μm (**a**) and (**c**) or 20 μm (**b**)

running along fibre edges. They extended processes towards the adjacent fibre area, crossing several fibres and appearing to terminate in contact with others. Clusters of KB cells grown on uncoated glass substrates did not have straight edges (Fig. 6c) and did not appear to be elongated in any particular direction. Cells growing throughout the cluster exhibited typical cobblestone epithelial morphology. Cells on the edges of clusters extended processes to contact the substrate. The length of processes was similar to those seen on fibre-coated substrates.

Image analysis data on the distribution of angles of cells on replicate samples were compared using pairwise comparisons of samples and two-sample Kolmogorov–Smirnov Z tests. Qualitative and quantitative analysis of the distributions suggested that replicate samples ($n = 3$) did not have significantly different ($P \leq 0.05$) distributions and therefore data for replicate samples were pooled for subsequent analysis. For HGF-1 studies this gave $n > 3{,}000$ and for KB, $n > 7{,}000$.

The distribution of angles of cells on untreated and plasma-treated fibre-coated substrates appeared to have a positive skew for HGF-1 (e.g. Fig. 7a, b), suggesting that the cells were oriented in the fibre direction. The distribution of angles of cells on uncoated glass substrates did not appear to show skew for either cell type (e.g. Fig. 7c, HGF-1), suggesting that the cells were randomly oriented. Skew and kurtosis values (Table 2) did not support these observations; only for untreated fibre-coated substrates at 7 days were skew and kurtosis >2, indicating deviation from normal distribution. It was noted that the number of cells oriented in the 0°, 45°, and 90° bins was lower than expected when compared to adjacent bins. This was investigated and determined to be an artefact of the image analysis system that did not affect overall data trends.

Figure 8 shows the percentage of cells oriented to within 20° of the measured direction for all substrates and time points. At all time points the percentage of HGF-1 cells oriented to within 20° of untreated and plasma-treated fibres was higher than the value predicted for a random uniform distribution (22.2%). The percentage of oriented cells on the uncoated substrates, however, remained similar to a uniform distribution. The percentage of oriented cells on untreated fibre-coated substrates was higher than that on the plasma-treated substrates at all time points and increased with time. Conversely, the percentage of oriented cells on plasma-treated substrates did not appear to increase significantly. These data support the observations made from qualitative assessment.

The mean shape ratio (ratio of width to length) was significantly lower ($P \leq 0.0025$) at 1 day on both types of fibre-coated substrate than on the uncoated substrates (Table 2). This trend was repeated at 4 and 7 days, with the exception that there was no significant difference between the shape ratio for cells on the plasma-treated fibre-coated substrates and uncoated substrates at 4 days. Furthermore, at 4 and 7 days the shape ratio was lower on the untreated fibre-coated substrate than the plasma-treated fibre-coated substrate. The mean shape ratio for all four substrate types significantly decreased ($P \leq 0.0025$) between 1 and 4 days. This may represent the spreading and adoption of

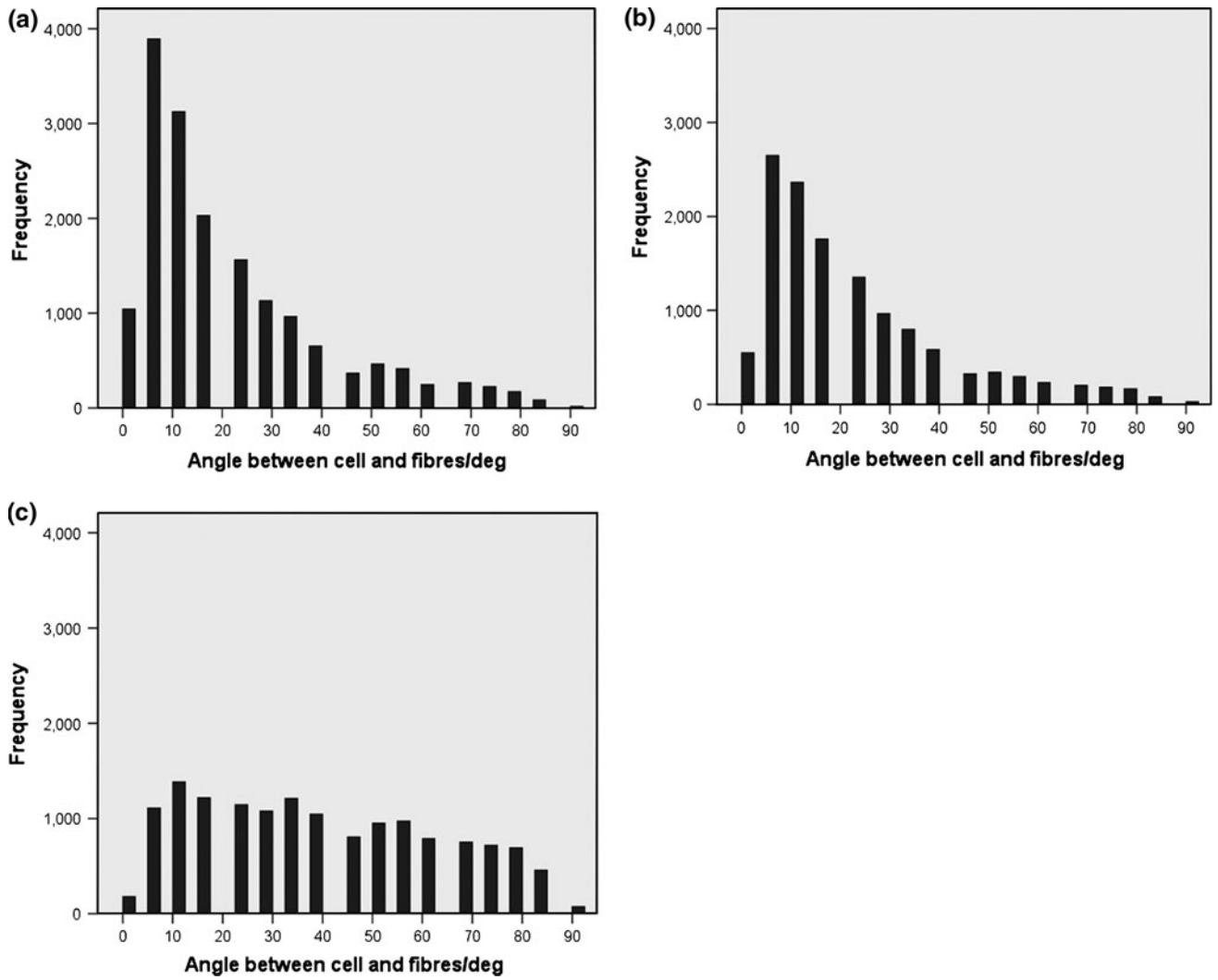

Fig. 7 Distribution of angles of HGF-1 cells grown for 4 days on (**a**) fibre-coated (**b**) plasma-treated fibre-coated and (**c**) uncoated substrates

bi-polar morphology seen with microscopy. Between 4 and 7 days, the shape ratio for cells on untreated and plasma-treated fibre-coated substrates decreased further, with the greatest decrease on the untreated substrate. Untreated and plasma-treated uncoated glass substrates did not show any decrease between 4 and 7 days. These data indicate that on fibre-coated substrates, individual cells and groups of cells become progressively more elongated. For groups of cells, this implies that cells were proliferating in one direction in preference to another.

Study of the coincidence of the shape ratio and angle of individual cells or cell clusters using scatter plots and the calculation of correlation coefficients suggests that cells oriented to the fibre direction were likely to have an elongated morphology, or that groups of cells were proliferating and migrating in one direction in preference to another. Statistically significant correlation coefficients ($P \leq 0.05$) were found for all substrates at all time points. The strength of the correlation on untreated, fibre-coated substrates increased with time. On plasma-treated, fibre-coated substrates, there was no real increase in the correlation coefficient; time did not affect the strength of the relationship between the two variables. The correlation coefficients on uncoated substrates were so low (an order of magnitude lower than those on fibre-coated substrates) that there was no meaningful correlation between the angle of orientation and the shape of individual cells or cell clusters. This is almost certainly due to the random orientation of the cells.

A further, shorter study was undertaken using KB cells. Data are summarised in Table 3. Although the distribution of the angles of cells appeared to be positively skewed on the fibre-coated substrates, skewness and kurtosis values did not support this observation. A higher percentage of cells were oriented to within 20° of the fibre direction than to the arbitrary direction on uncoated substrates and than expected for a uniform distribution. On both types of

Table 2 Summary of image analysis statistics for HGF-1 cells grown on test substrates for 1, 4 and 7 days

Time (days)	Substrate type	Skew of angle of cell orientation	Kurtosis of angle of cell orientation	Shape ratio (width:length)	Correlation between cell orientation and shape ratio ($P \leq 0.05$)
1	Fibres	0.782 (0.04)	−0.367 (0.07)	0.503 (≤0.01)	0.402
	Plasma fibres	0.674 (0.05)	−0.543 (0.09)	0.480 (≤0.01)	0.296
	Uncoated	0.187 (0.04)	−1.096 (0.07)	0.534 (≤0.01)	0.030
	Plasma uncoated	0.336 (0.04)	−0.996 (0.09)	0.554 (≤0.01)	0.058
4	Fibres	1.051 (0.04)	0.143 (0.09)	0.336 (≤0.01)	0.501
	Plasma fibres	0.516 (0.04)	−0.807 (0.08)	0.387 (≤0.01)	0.274
	Uncoated	0.118 (0.04)	−1.144 (0.09)	0.402 (≤0.01)	0.073
	Plasma uncoated	0.208 (0.04)	−1.093 (0.08)	0.389 (≤0.01)	0.038
7	Fibres	2.140 (0.04)	4.711 (0.07)	0.278 (≤0.01)	0.665
	Plasma fibres	0.763 (0.04)	−0.430 (0.07)	0.358 (≤0.01)	0.311
	Uncoated	0.135 (0.03)	−1.095 (0.07)	0.399 (≤0.01)	0.085
	Plasma uncoated	0.160 (0.04)	−1.113 (0.08)	0.392 (≤0.01)	0.064

Mean values (standard error in parentheses), $n = 3$

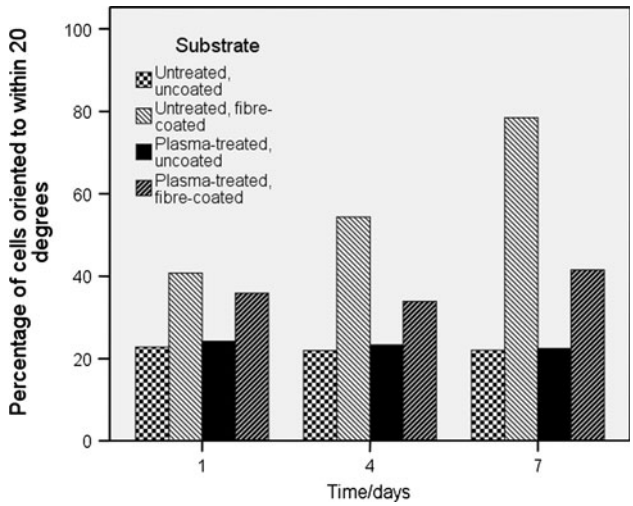

Fig. 8 Percentage of HGF-1 cells oriented to within 20° of measured direction on different substrates

substrate, there was a low frequency of cells in the 0°–10° bin. As discussed above, this is an artefact of the software and may account for the fact that the proportion of oriented cells was low on the uncoated substrates. The shape ratio of the cells was statistically lower (independent samples *t* test, equal variances not assumed, $P \leq 0.001$) on fibre-coated substrates than on the uncoated substrates. Study of the coincidence of the shape ratio and angle of orientation indicated that, on fibre-coated substrates, oriented cells or clusters were more elongated than those that were not oriented. This was confirmed by a statistically significant correlation ($P \leq 0.05$) between the variables and supports the qualitative observations (e.g. Fig. 6). Cells on uncoated substrates did not show a trend in terms of cell orientation and shape ratio. Although a statistically significant correlation was found, the coefficient was so low that it does not suggest any meaningful relationship between the angle of orientation and cell morphology.

4 Discussion

The influence of substratum nanotopography and chemistry on cellular response has been well reported, and has been shown to affect cell adhesion, orientation and differentiation. Control or manipulation of cellular response is important for a variety of biomaterial applications. In this study, a relatively simple method of producing surfaces with nanoscale topography and different surfaces chemistries

Table 3 Summary of image analysis statistics for KB cells grown for 4d

Substrate type	Skew of angle of cell orientation	Kurtosis of angle of cell orientation	Percentage of objects oriented within 20°	Shape ratio (width:length)	Correlation between cell orientation and shape ratio ($P \leq 0.05$)
Fibres	0.615 (0.03)	−0.595 (0.06)	31.54	0.558 (≤0.01)	0.408
Uncoated	0.145 (0.03)	−1.067 (0.05)	16.19	0.607 (≤0.01)	0.058

Mean values (standard error in parentheses)

was used to elucidate the effect and interaction of these two surface features on cellular response in vitro.

Previous studies have demonstrated that friction transfer of PTFE produces nanoscale features on a substrate under appropriate manufacturing conditions. Our studies confirmed that the substrate temperature had a significant influence on the nature of the deposited PTFE [15], with increased temperature resulting in denser packing of fibres. Insufficient pressure resulted in the formation of wavy fibres, however once the pressure was high enough to form straight, continuous fibres, a further increase did not appear to affect fibre spacing or widths. These data may support reports that increased pressure increases coverage and decreases variations in the coating [12–14]. The effect of sliding speed was not systematically investigated; the conditions used here resulted in a low friction regime in which speed has been reported to have little influence on the PTFE coating as long as it was constant [12–14].

White light interferometry is a technique that allows rapid analysis of surface topography, which gives it a practical advantage over AFM when used to study a large number of substrates. The vertical resolution is nominally 3 nm for a highly reflective surface such as that studied here. The dense packing of the fibres meant that other surface profiling techniques such as AFM may also 'under'-measure fibres as the tip would be unable to reach between two closely-packed fibres. Studies of the same surfaces with AFM and light interferometry yielded similar results, with slightly more noise in the interferometry data. Three-dimensional plots always showed fibres in areas where fibres were expected, whereas uncoated glass surfaces appeared relatively flat. Analysis of individual height profiles to calculate surface roughness statistics such as R_a and R_q, however, did not consistently show a statistically significant difference between fibre-coated and uncoated glass substrates. The influence of noise, particularly on R_{ku}, may be detrimental when features are on the nanoscale. Furthermore, surface roughness statistics are not always able to discriminate between topographies where feature heights and spacing are very different. This suggests that the use of these surface roughness statistics to describe and compare nanotopography may be insufficient to describe the surface accurately.

It has been demonstrated previously that surface chemistry and topography can affect cellular response. In addition to the topography they produced, the hydrophobic PTFE fibres presented a very different surface chemistry to cells compared with the relatively hydrophilic glass substrates. Ammonia plasma treatment was used to defluorinate the PTFE fibres, as demonstrated by XPS, in an attempt to reduce the difference in hydrophilicity between fibres and underlying substrate. In the study by Coen et al. [25], PTFE fibrils were observed to be reduced in width from 200–300 nm to 100–200 nm following a 2 min helium plasma treatment, with the rate of etching being estimated as 30–50 nm min^{-1}. The data from our studies suggest that the fibre coating was unaffected in terms of fibre distribution or morphology. The post-treatment reaction in water resulted in the incorporation of hydrophilic O-containing groups, shown by the broadening of the carbon peak. These moieties may include C=O, C–O, O–C=O, C–H and C–N [17, 26, 27].

Confirmation of the increased hydrophilicity from incorporation of polar groups was obtained by DCA analysis, which demonstrated a significant decrease in advancing and receding angles following the post-treatment reaction. It is important to consider the effect that the fibre coating had on the measured contact angles. The motion of a contact line as a liquid spreads across a surface can be impeded by physical or chemical heterogeneities, a phenomenon termed 'pinning'. Pinning forces depend on, amongst other factors, the chemical strength of the features on chemically heterogeneous surfaces [28]. The rate of liquid spread across corrugated surfaces can be enhanced by surface or chemical patterning. This 'wicking' is proportional to the groove depth or diameter [29] and has been observed on smooth surfaces patterned with chemical hydrophilic and hydrophobic regions [30]. When the PTFE fibres studied here were oriented horizontally, and so the liquid was presented with the chemical and topographical barrier of the fibres, the constant change in force due to pinning made it impossible to calculate contact angle. Vertical orientation of fibres allowed a contact angle to be derived, although the data may have been influenced by the wicking effect. The water may have spread preferentially in the fibre direction, i.e. vertically, due to capillary forces. The plasma treatment may have reduced the relative difference between the fibres and the underlying substrate, resulting in increased horizontal liquid spreading. The lateral resolution of DCA analysis technique is approximately 1 mm [31], several orders of magnitude above that of the features being produced by friction transfer. This means that when surfaces with heterogeneous chemistry or topography, such as those studied here, are being investigated, the contact angles calculated will be the mean values for the whole surface, not distinguishing between different domains. The accuracy of the measurements may also have been reduced due to the use of double-thickness substrates, which may also have been subject to wicking between the two substrates, making it difficult to compare the data obtained in this study with other work. Unfortunately the nature of the surface coating procedure employed in this study means that it is impossible to manufacture a single-thickness substrate with the fibre coating on both sides.

In this study both fibroblast and epithelial cell types responded to the PTFE fibre coating in terms of their orientation. Individual cells were elongated such that their

major axis was parallel to the fibre direction. Clusters of cells appeared to spread in the fibre direction to a greater extent than perpendicular to the fibres, as shown by image analysis. Cell morphology was also observed to alter in response to the fibre coatings, with many cells becoming more elongated than on uncoated substrates. The morphology of epithelial cells on fibre-coated substrates was dependent on whether the cell was growing individually or in a cluster. Individual epithelial cells exhibited a non-native, elongated shape on fibre-coated substrates whereas the morphology of epithelial cells growing in clusters on fibre-coated substrates was not affected by the fibres, even though the clusters themselves were elongated in the fibre direction. Cells at the edges of the clusters, however, were observed to be affected by the fibres. These findings are in agreement to those reported by Clark et al. [32], although in that study the features were two orders of magnitude greater in height and at least one order of magnitude larger in the lateral dimensions. Other work, however, suggested that epithelial cells in clusters adopted the greatest alignment to surface topography [33]. Fibroblasts with bipolar morphology were observed on fibre-coated and uncoated substrates. Orientation of individual fibroblast cells has been reported to decrease at longer time points, when more cells are in contact with each other [34]. In our studies, this did not appear to be the case, with a high proportion of cells remaining elongated parallel to the fibres after 10 days despite extensive cell–cell contact. Ammonia plasma treatment of the fibres caused fewer cells to orient compared to cells in contact with untreated fibres. Additionally, image analysis indicated that, for gingival fibroblasts, whereas on untreated fibre-coated surfaces the proportion of oriented cells increased with time, on plasma-treated fibres, there was a plateau in the proportion of oriented cells. Cells and cell clusters on plasma-treated fibres were also less elongated than on the untreated fibres, although more elongated than on uncoated surfaces. These results suggested that although topography can cause orientation of cells, the surface chemistry had an effect on the extent of orientation. Other researchers have indicated that the effect of surface topography can overcome that of a competing surface chemistry [35, 36], suggesting that it may be the stronger influence on cell behaviour.

The PTFE fibre coating appeared to restrict the direction of cell spreading. Epithelial cells did not encroach onto areas covered by fibres but spread preferentially parallel to the fibre direction, suggesting the fibres act as an impediment to cell migration. Similar findings have been reported by Teixeira et al. [37], who propose that restriction of lateral spreading of epithelial cells is due to the failure of lamellipodia to span grooves.

The various theories into cellular response to substratum topography have been discussed by many other authors. Important physical factors are the shape and aspect ratio of the features [38], which may affect cell cytoskeleton and hence migration and other functions. In vitro culture conditions also play a part [37], primarily by changing protein adsorption onto the surface. Localised differences in protein adsorption are also important in controlling the cellular response to patterns of surface chemistry. Patterning with hydrophobic surface chemistries, such as that of the PTFE fibres used in this study, has been demonstrated to result in a surface that restricts cell migration [39]. Topography can also alter the conformation of adsorbed protein. F-actin has been reported to adsorb and orient onto ridges with 1 nm height and 40 nm width, whereas on similar structures with 4 nm heights, or flat surfaces, adsorption was lower and orientation random [40]. Furthermore, it has been demonstrated that adsorption of proteins onto nano-rough surfaces leads to a masking of the surface features [41]. The combination of a pattern of surface chemistry and topography is also important. Denis et al. [41] showed that the surface chemistry of a nano-rough substrate affected the amount of protein adsorbed, whereas the surface topography modulated its organisation, although it has also been reported that initial protein adsorption is not affected by surface chemistry [42]. In our studies, surface chemistry appeared to modulate the extent to which cells oriented to the surface features demonstrating that in this particular case both the chemistry and topography had a significant influence on the cell behaviour. There may be an argument that the extent of the influence on cell behaviour depends on the specifics of the topographical features and the chemistry.

The use of chemical and topographical patterning contributes towards the understanding of cellular interaction with biomaterials and may, in the longer term, help to improve the performance of medical devices. At a protein level, the control of protein conformation and orientation has been demonstrated to be an important factor in controlling the response to implanted biomaterials, particularly at the cell signalling level [43]. The control of orientation and migration of cells may be useful in a variety of tissue engineering applications, particularly in neural regeneration [44] and at the tissue-implant interface. This technology is currently under investigation in the field of dental implants. The component of the implant that is in contact with oral epithelium before it enters the bone needs to resist epithelial downgrowth so as not to compromise the bone-implant interface and often has machining grooves on the abutment that are designed to facilitate this and improve the soft tissue attachment [45, 46]. Biomaterial surface patterning and topography may also be used to control cell differentiation [8] and biofouling.

One significant advantage of the friction transfer process is that it is a relatively inexpensive method of producing surface nanotopography compared to procedures such as

electron beam lithography. A potential disadvantage is that the dimensions of the features vary, in comparison to techniques that produce a more well-defined pattern. Techniques that produce non-uniform features, however, are relatively common with medical devices; well-defined patterns are more commonly used for research into cellular response. It may be that as long as the features fall within a certain size range, all sub-500 μm, for example, the in vivo cellular response will be consistent. The requirement to heat the substrate to achieve controlled, nanoscale features means that this technique is unsuitable for modification of polymer substrates. The model glass substrates used here were smooth. It remains to be seen whether friction transfer would produce controlled nanotopography on rougher substrates and how these would influence the cellular response. Additionally, the use of coatings on medical devices may be undesirable, particularly in the light of well-publicised device failures where the coating has come detached from the underlying substrate. Nevertheless, this technique does demonstrate that the features produced by friction transfer of PTFE modulate cellular response in vitro.

5 Conclusions

Friction-transfer of PTFE can produce nanoscale features. These features have been demonstrated to affect fibroblast and epithelial cell responses in terms of orientation and migration in vitro. The nanofeatures present the cells with a modified chemistry and topography. Plasma treatment defluorinates the PTFE fibres, which continue to modulate the cellular response, although to a lesser extent. This demonstrates that chemistry and topography are important cell regulatory factors on these substrates.

Acknowledgments The financial support of Friadent GmbH, Health Technologies Knowledge Transfer Network and EPSRC are gratefully acknowledged. The authors would also like to thank Sandra Fawcett for assistance with SEM and Dr David Martin for operation of the AFM.

References

1. Flemming RG, Murphy CJ, Abrams GA, Goodman SL, Nealey PF. Effects of synthetic micro- and nano-structured surfaces on cell behavior. Biomaterials. 1999;20:573.
2. Curtis A, Wilkinson C. Topographical control of cells. Biomaterials. 1997;18:1573–83.
3. Jung DR, Kapur R, Adams T, Giuliano KA, Mrksich M, Craighead HG, et al. Topographical and physicochemical modification of material surface to enable patterning of living cells. Crit Rev Biotechnol. 2001;21:111–54.
4. Nagaoka S, Ashiba K, Kawakami H. Biomedical properties of nanofabricated fluorinated polyimide surface. Artif Organs. 2002;26:670–5.
5. Andersson AS, Olsson P, Lidberg U, Sutherland D. The effects of continuous and discontinuous groove edges on cell shape and alignment. Exp Cell Res. 2003;288:177–88.
6. Zhu B, Zhang Q, Lu Q, Xu Y, Yin J, Hu J, et al. Nanotopographical guidance of C6 glioma cell alignment and oriented growth. Biomaterials. 2004;25:4215–23.
7. Cousins BG, Doherty PJ, Williams RL, Fink J, Garvey MJ. The effect of silica nanoparticulate coatings on cellular response. J Mater Sci Mater Med. 2004;15:355–9.
8. Dalby MJ, Gadegaard N, Tare R, Andar A, Riehle MO, Herzyk P, et al. The control of human mesenchymal cell differentiation using nanoscale symmetry and disorder. Nat Mater. 2007;6:997–1003.
9. Jung YL, Donahue HJ. Cell sensing and response to micro- and nanostructured surfaces produced by chemical and topographic patterning. Tissue Eng. 2007;13:1879–91.
10. Curtis A. The potential for the use of nanofeaturing in medical devices. Expert Rev Med Devices. 2005;2:293–301.
11. Kearns VR, McMurray RJ, Dalby MJ. Surface topography to control cellular response. In: Williams RL, editor. Surface modification of biomaterials: methods, analysis and applications. Cambridge: Woodhead Publishing Limited; 2010 (In press).
12. Bodo P, Schott M. Highly oriented polytetrafluoroethylene films: a force microscopy study. Thin Solid Films. 1996;286:98.
13. Beamson G, Clark DT, Deegan DE, Hayes NW, Law DSL, Rasmusson JR, et al. Characterization of PTFE on silicon wafer tribological transfer films by XPS, imaging XPS and AFM. Surf Interface Anal. 1996;24:204–10.
14. Fenwick D, Ihn KJ, Motamedi F, Wittmann JC, Smith P. Characterization of friction-deposited polytetrafluoroethylene transfer films. J Appl Polym Sci. 1993;50:1151–7.
15. Pooley CM, Tabor D. Friction and molecular structure: the behaviour of some thermoplastics. Proc R Soc Lond A. 1972;329:251–74.
16. Jain VK, Bahadur S. Material transfer in polymer-polymer sliding. Wear. 1978;46:177–88.
17. Markkula TK, Hunt JA, Pu FR, Williams RL. Surface chemical derivatization of plasma-treated PET and PTFE. Surf Interface Anal. 2002;34:583–7.
18. Wilson DJ, Williams RL, Pond RC. Plasma modification of PTFE surfaces Part II: plasma-treated surfaces following storage in air or PBS. Surf Interface Anal. 2001;31:397–408.
19. Pringle SD, Joss VS, Jones C. Ammonia plasma treatment of PTFE under known plasma conditions. Surf Interface Anal. 1996;24:821–9.
20. Suzuki H, Oiwa K, Yamada A, Sakakibara H, Nakayama H, Mashiko S. Linear arrangement of motor protein on a mechanically deposited fluoropolymer thin-film. Jpn J Appl Phys Part 1. 1995;34:3937–41.
21. Rasmusson JR, Erlandsson R, Salaneck WR, Schott M, Clark DT, Lundstrom I. Adsorption of fibrinogen on thin oriented poly(tetrafluoroethylene) (Ptfe) fibers studied by scanning force microscopy. Scanning Microsc. 1994;8:481–90.
22. Wilson DJ, Williams RL, Pond RC. Plasma modification of PTFE surfaces Part I: surfaces immediately following plasma treatment. Surf Interface Anal. 2001;31:385–96.
23. Beamson G, Briggs D, Davies SF, Fletcher IW, Clark DT, Howard J, et al. Performance and application of the Scienta ESCA300 spectrometer. Surf Interface Anal. 1990;15:541–9.
24. Gelius U, Wannberg B, Baltzer P, Fellnerfeldegg H, Carlsson G, Johansson CG, et al. A new ESCA instrument with improved surface sensitivity, fast imaging properties and excellent energy resolution. J Electron Spectrosc Relat Phenom. 1990;52:747–85.
25. Coen MC, Lehmann R, Groening P, Schlapbach L. Modification of the micro- and nanotopography of several polymers by plasma treatments. Appl Surf Sci. 2003;207:276–86.

26. Nakamatsu J, Delgado-Aparicio LF, Da Silva R, Soberon F. Ageing of plasma-treated poly(tetrafluoroethylene) surfaces. J Adhes Sci Technol. 1999;13:753–61.
27. Koenig U, Nitschke M, Pilz M, Simon F, Arnhold C, Werner C. Stability and ageing of plasma treated poly(tetrafluoroethylene) surfaces. Colloids Surf B Biointerfaces. 2002;25:313–24.
28. de Gennes PG. Wetting: statics and dynamics. RvMP. 1985; 57:827.
29. Rye RR, Mann JA, Yost FG. The flow of liquids in surface grooves. Langmuir. 1996;12:555–65.
30. Darhuber AA, Troian SM, Reisner WW. Dynamics of capillary spreading along hydrophilic microstripes. PhRvE. 2001;6403: 316031–8.
31. Ratner BD. Surface properties of materials. In: Ratner BD, et al., editors. Biomaterials science: an introduction to materials in medicine. San Diego: Academic Press; 1996.
32. Clark P, Connolly P, Curtis AS, Dow JA, Wilkinson CD. Topographical control of cell behaviour: II. Multiple grooved substrata. Development. 1990;108:635–44.
33. Oakley C, Brunette DM. The sequence of alignment of microtubules, focal contacts and actin filaments in fibroblasts spreading on smooth and grooved titanium substrata. J Cell Sci. 1993;106: 343–54.
34. den Braber ET, de Ruijter JE, Ginsel LA, von Recum AF, Jansen JA. Orientation of ECM protein deposition, fibroblast cytoskeleton, and attachment complex components on silicone microgrooved surfaces. J Biomed Mater Res. 1998;40:291–300.
35. Charest JL, Eliason MT, García AJ, King WP. Combined microscale mechanical topography and chemical patterns on polymer cell culture substrates. Biomaterials. 2006;27:2487–94.
36. Yim EK, Reano RM, Pang SW, Yee AF, Chen CS, Leong KW. Nanopattern-induced changes in morphology and motility of smooth muscle cells. Biomaterials. 2005;26:5405–13.
37. Teixeira AI, Abrams GA, Bertics PJ, Murphy CJ, Nealey PF. Epithelial contact guidance on well-defined micro- and nanostructured substrates. J Cell Sci. 2003;116:1881–92.
38. Crouch AS, Miller D, Luebke KJ, Hu W. Correlation of anisotropic cell behaviors with topographic aspect ratio. Biomaterials. 2009;30:1560–7.
39. Britland S, Clark P, Connolly P, Moores G. Micropatterned substratum adhesiveness: a model for morphogenetic cues controlling cell behavior. Exp Cell Res. 1992;198:124–9.
40. Galli C, Collaud Coen M, Hauert R, Katanaev VL, Wymann MP, Groning P, et al. Protein adsorption on topographically nanostructured titanium. Surf Sci. 2001;474:L180–4.
41. Denis FA, Hanarp P, Sutherland DS, Gold J, Mustin C, Rouxhet PG, et al. Protein adsorption on model surfaces with controlled nanotopography and chemistry. Langmuir. 2002;18:819–28.
42. Sutherland DS, Marita B, Hakan N, Bengt K. Influence of nanoscale surface topography and chemistry on the functional behaviour of an adsorbed model macromolecule. Macromol Biosci. 2001;1:270–3.
43. Castner DG, Ratner BD. Biomedical surface science: foundations to frontiers. Surf Sci. 2002;500:28–60.
44. Miller C, Jeftinija S, Mallapragada S. Micropatterned Schwann cell-seeded biodegradable polymer substrates significantly enhance neurite alignment and outgrowth. Tissue Eng. 2001;7: 705–15.
45. Chehroudi B, Gould TR, Brunette DM. Titanium-coated micromachined grooves of different dimensions affect epithelial and connective-tissue cells differently in vivo. J Biomed Mater Res. 1990;24:1203–19.
46. Kim H, Murakami H, Chehroudi B, Textor M, Brunette DM. Effects of surface topography on the connective tissue attachment to subcutaneous implants. Int J Oral Maxillofac Implants. 2006; 21:354–65.